JOURNAL OF NANO- AND ELECTRONIC PHYSICS
Vol. **7** No 4, 04037(4pp) (2015)

ЖУРНАЛ НАНО- ТА ЕЛЕКТРОННОЇ ФІЗИКИ
Том **7** № 4, 04037(4cc) (2015)

Synthesis of Nanostructured Tin Oxide (SnO_2) Powders and Thin Films Prepared by Sol-Gel Method

Ashok D. Bhagwat[1,2], Sachin S. Sawant[1], Balaprasad G. Ankamwar[3], Chandrashekhar M. Mahajan[1,*]

[1] *Department of Engineering Sciences and Humanities, Vishwakarma Institute of Technology, Pune – 411037, Maharashtra, India*
[2] *Dnyanshree Institute of Engineering and Technology, Satara – 415013, Maharashtra, India*
[3] *Department of Chemistry, Savitribai Phule Pune University, Ganeshkhind, Pune, 411007, India*

(Received 09 July 2015; revised manuscript received 08 December 2015; published online 10 December, 2015)

Nanocrystalline SnO_2 powder was successfully prepared by using simple sol-gel technique. The sol-gel obtained was washed and calcinated at 400 °C to obtain the SnO_2 nano-powder. The structural property of (SnO_2) nanocrystalline powder was investigated by using X-ray diffraction (XRD) technique. The optical properties were studied using Uv-Vis Spectroscopy, by recording the absorbance and transmittance spectra. The XRD pattern of the as-prepared sample demonstrated the formation of a rutile structure of SnO_2 nanocrystallites. The Scanning Electron Microscopic (SEM) analysis showed a homogeneous distribution of quite small grains over scanned area. The Uv-Vis absorbance spectra also showed a characteristic peak of absorbance at $\lambda = 312$ nm corresponding to SnO_2. The energy band gap measurement for nanocrystalline SnO_2 thin film was done from the graph of variation of $(\alpha h\nu)^2$ versus $h\nu$. The measured value of optical bandgap energies for SnO_2 thin film is 3.78 eV. The results show that the transmittance of the synthesized SnO_2 film is 78 % in the spectral range 350 nm to 800 nm.

Keywords: Bandgap, Metal oxide, Tin oxide, nanocrystallites, Sol-gel.

PACS numbers: 61.05.C, 61.82.Rx, 68.37.Hk, 81.20.Fw

1. INTRODUCTION

Nano-crystals of semiconductor metal oxides have attracted a great interest due to their intriguing properties, which are different from those of their corresponding bulk state. Tin Oxide (SnO_2) is one of the important metal oxides due to its many useful properties such as its wide band gap ($E_g = 3.64$ eV, 330 K), *n*-type conductivity, high transparency in the visible range (> 80 %). It crystallizes in rutile structure and can be synthesized in variety of shapes and sizes using different low cost synthesis techniques relevant for a wide range of applications such as in solid-state gas sensors, flat panel displays, solar energy cells [1, 2]. The thin films of SnO_2 shows high free carrier density in the range of 10^{19}-10^{20} cm^{-3} which is mainly due to oxygen vacancies, incorporation of excess interstitial tin and unintentional chlorine doping (mainly from glass substrates at higher deposition or calcination temperatures due to softening of soda lime glass).

Various impressive and effective methods have been used to prepare SnO_2 nanostructures with better control over particle size and physical properties. These includes hydrothermal method [3, 4], polymeric [5], organo-metallic precursor synthesis [6], sonication [7, 8], microwave [9, 10] and surfactant-mediated method [11]. However, they are either complicated, costly and energy or time-consuming. It takes at least 24hrs. for the hydrothermal method to synthesize SnO_2 nanoparticles. Besides, the polymeric and sonication techniques are complicated and give fewer throughputs, hence are not favorable for mass production. Conversely, sol-gel is a simple technique to synthesize homogeneous nanoparticles of high purity and crystallinity at a low temperature. In a sol-gel process, the precursor solution is transformed into an inorganic solid by (a) dispersion of colloidal particles in a liquid (sol) and (b) conversion of sol into rigid phase (gel) by hydrolysis and condensation reactions [12]. Generally it leads to synthesis of amorphous precipitates and heat treatment is necessary to induce particle growth by re-crystallization and to alter the particle morphology. However, amongst different synthesis methods for preparation of tin oxide, sol gel method offers several advantages over other methods in terms of lower processing temperature, better homogeneity and controlled stoichiometry, flexibility of forming dense monoliths, thin films, and nanoparticles. In the present work we have investigated the structural, morphological and optical properties of SnO_2 nano-powder and thin film synthesized by simple and facile sol-gel technique. The properties of these SnO_2 nanocrystallites have been studied using different characterization techniques such as X-ray diffraction (XRD), Scanning Electron Microscopy (SEM), UV-VIS spectroscopy.

2. EXPERIMENTAL

2.1 Materials

Analytical Reagent (A.R.) grade chemicals such as tin tetrachloride penta-hydrate ($SnCl_4.5H_2O$), ethylene glycol and ammonia (Make: Loba Chemie Pvt. Ltd. Mumbai, India), were used for synthesis of SnO_2 nanoparticles without any further purification. The double distilled water was used during the synthesis as a solvent for precursors such as $SnCl_4.5H_2O$, ethylene glycol and liquid ammonia.

* c_mahajan9@yahoo.com

2.2 Method

The sol-gel technique was used for the synthesis of tin oxide nano-powder. The 0.1 molar of tin-tetrachloride penta-hydrate (3.51 g of $SnCl_4.5H_2O$) was dissolved in 50 ml of double distilled water in a beaker to which 50 ml of ethylene glycol was added to make a 100 ml precursor mixture. The resulted precursor mixture was kept for stirring on a magnetic stirrer (Make: Remi) at 300 RPM and while stirring into this mixture, 0.1M of an aqueous ammonia solution was added in drop wise manner (with a rate of 10 drops/minute). On addition of roughly 50 drops of aqueous ammonia the sol-gel was formed approximately within the 5 minutes. The resulting gel was filtered by using Whatman filter paper (grade-42) and then washed 3-4 times by double distilled water to remove excess ammonia. The content on the filter paper was then transferred carefully in a crucible as well as on a glass substrate with 1 μm commercial applicator to form a thin film. The precipitate in the crucible and a thin film was dried at 150 ºC for 2 hrs. in order to remove water molecules. Finally, black brown colored tin oxide nano-powder was obtained for a crucible sample and a film on glass substrate after drying, were further calcinated at 400 ºC for 2 hrs. [13]. Fig. 1 shows the Photographic illustration of different steps involved in synthesis process of SnO_2 nanocrystallites by sol-gel method.

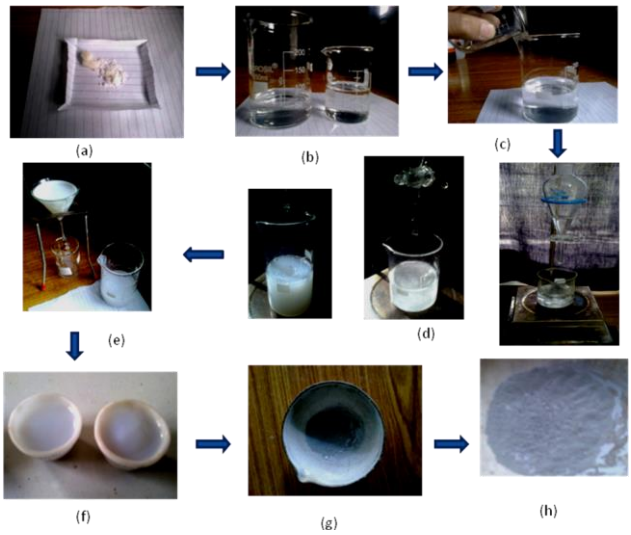

Fig. 1 – Stepwise photographic illustration of synthesis process of SnO_2 nanocrystallites (a) precursor, $SnCl_4.5H_2O$, (b) solutions in beakers contain from left to right $SnCl_4.5H_2O$, ethylene glycol, (c) simultaneous addition, (d) gel formed by drop-wise addition aqueous ammonia under constant magnetic stirring, (e) filtration and washing, (f) gel of SnO_2 nanocrystallites, (g) dried SnO_2 nanocrystallites at 150 ºC for 2 hrs. and (h) calcinated at 400 °C to obtain SnO_2 nanocrystallites in powder form

2.3 Characterization

The structural properties of SnO_2 nano-powder were studied by X-ray diffraction measurements (Bruker D-8 advance diffractometer, Billerica, MA) using the Cu Kα ($\lambda = 1.5406$ Å) as a radiation source, operated at 40kV and 30 mA with a scan rate of 0.02°/s over the range of 10°-80°. The average crystallite size d(hkl) of all crystal planes for SnO_2 powder was estimated from the classical Scherrer formula [14]:

$$D = \frac{K\lambda}{\beta \cos\theta} \quad (1)$$

where K is the shape factor usually has a value 0.9, λ is the X-ray wavelength and θ the Bragg angle and β gives the full width of the half maxima (FWHM).

The surface morphology of the SnO_2 powder was studied by scanning electron microscope (SEM). The spectral transmittance and absorbance measurements were obtained using UV-VIS spectrometer (Shimatzu 1650PC) in the spectral range of 250 nm to 800 nm. The X-intercept obtained by extrapolating the linear portion of the exponential curve from of the graph of ($\alpha h\nu^2$) versus photon energy ($h\nu$) is the bandgap energy of the material.

3. RESULTS AND DISCUSSIONS

3.1 Structural and Morphological Properties

The powder X-ray diffraction analysis of the SnO_2 sample was performed in order to identify the phase, crystal structure and to estimate average grain size. The as recorded X-ray diffraction pattern of SnO_2 powder sample by sol-gel technique is as presented in Fig. 2. The XRD pattern reveals the formation of SnO_2 nanoparticles with polycrystalline phase demonstrating rutile structure [JCPDS Card No: 41-1445, $a = 4.743$ Å. $c = 3.1859$ Å]. The crystal planes (110), (101), (211), (002), (310), (301) were prominently seen in XRD indicating the polycrystalline nature of powder. The average value of lattice constant from different (hkl) planes was determined by using the formula, $a = d\sqrt{h^2 + k^2 + l^2}$ where d is inter-planer distance and (hkl) are Miller indices. The calculated average values of lattice constant were $a = 4.7470$ Å, $c = 3.1854$ Å. No impurity phase was observed. The average crystallite size (D) as determined from the XRD spectra using Scherer's formula was 52 nm. The respective angles of peak positions (2θ), hkl planes and inter-planar distance (d) are represented in Table 1.

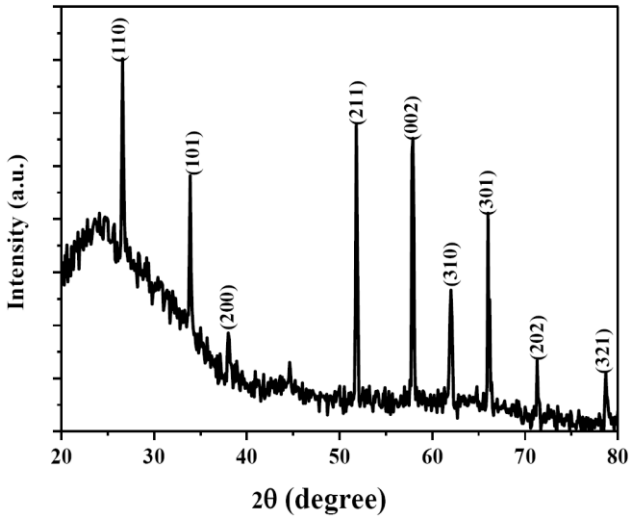

Fig. 2 – XRD pattern of SnO_2 nanocrystallites

Table 1 – XRD analysis of SnO_2 nanocrystallites

2θ	(*hkl*) planes	Inter-planar distances (*d*) in nm
26.6⁰	(110)	58.9
33.9⁰	(101)	55.3
38.0⁰	(200)	43.6
51.8⁰	(211)	59.3
57.9⁰	(002)	57.7
62.0⁰	(310)	49.3
66.0⁰	(301)	51.7
71.3⁰	(202)	47.5
78.7⁰	(321)	44.4

SEM analysis was performed to reveal morphological features of the sample. SEM micrograph of nanocrystalline SnO_2 thin film is shown in Fig. 3. Fig. 3 shows a homogeneous, uniform distribution of SnO_2 nanocrystallines over a scanned area.

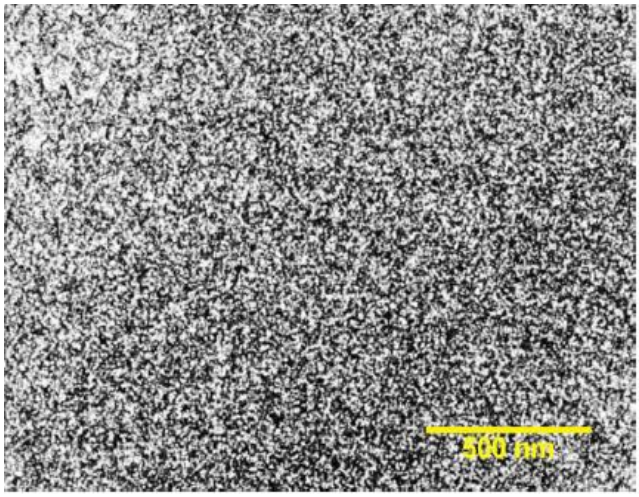

Fig. 3 – SEM micrograph of SnO_2 nanocrystallites

3.2 Optical Properties

The UV-VIS absorbance spectra of SnO_2 nanocrystallites are as represented in the Fig. 5. The characteristic absorption peak was found around 312 nm in the region (275 nm $\leq \lambda \leq$ 350 nm). The substantial decrease in transmittance for SnO_2 nanocrystallites near the band edge indicates the better crystallinity and lower defect density for synthesized thin film.

The analysis of the transmission Fig. 4 (thin film) and absorbance spectra (absorbance for SnO_2 nanocrystallites sample) in the vicinity of the fundamental absorption edge shows that the variation of the absorption coefficient is in accordance with following relation which implies the direct transitions [15].

$$(\alpha h\nu)^2 = \mathrm{A}(h\nu - \mathrm{E}_g) \qquad (2)$$

Here, α is an absorption coefficient, h is Planck constant, ν is the frequency and $h\nu$ is the incident photon energy. Fig. 6 represents the plot of $(\alpha h\nu)^2$ vs $h\nu$ for SnO_2 nanocrystallites.

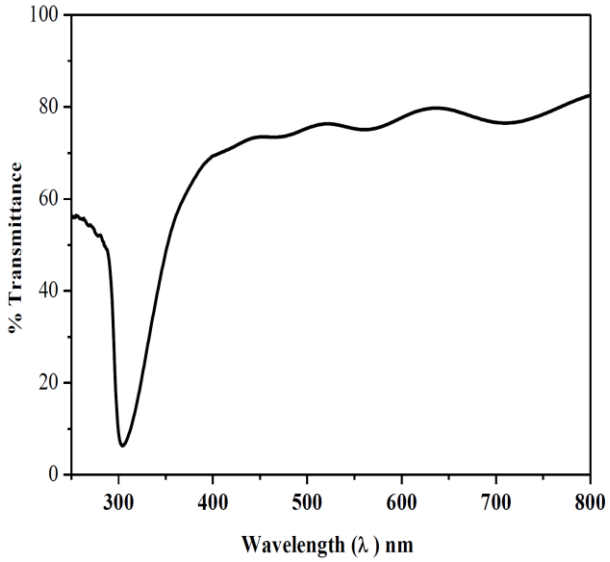

Fig. 4 – Transmittance spectrum of SnO_2 thin film

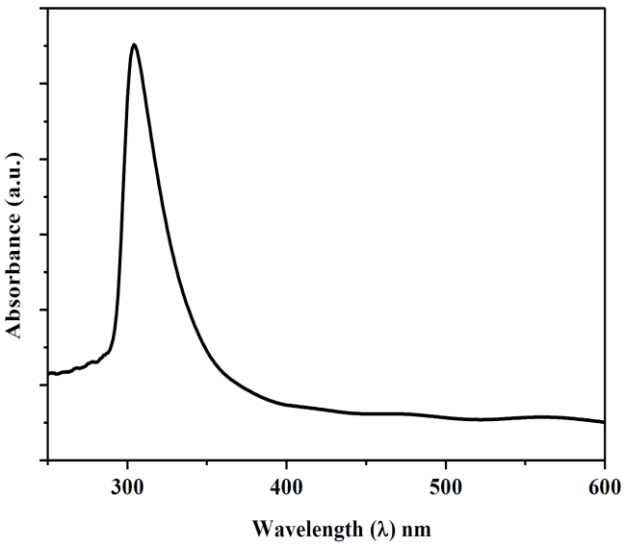

Fig. 5 – UV-VIS absorption spectrum of SnO_2 nanocrystallites

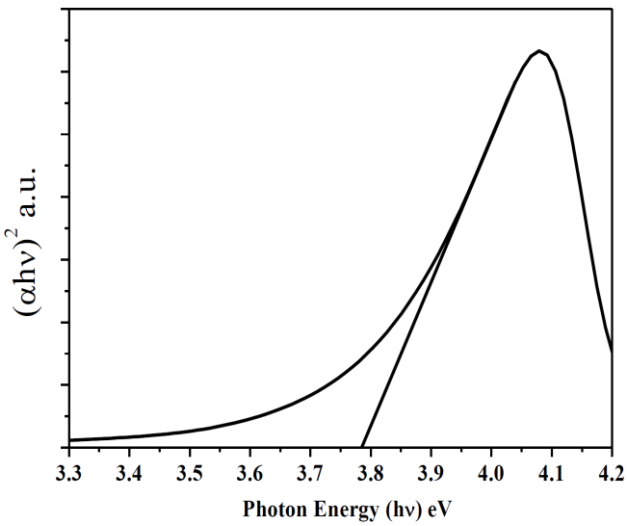

Fig. 6 – The plot of $(\alpha h\nu)^2$ vs $h\nu$ for SnO_2 nanocrystallites

The direct band gap (E_g) of our sample was measured from the absorption coefficient data as a function of wavelength using Tauc relation thereby extrapolating the straight line of the $(\alpha h\nu)^2$ vs. $h\nu$ plot to intercept on the horizontal photon energy axis and was found to 3.78 eV as shown in Fig. 6. It is clear that the obtained tin oxide has the optical band gap larger than the value of 3.64 eV for bulk SnO_2 [16] which can be attributed to quantum confinement effect.

4. CONCLUSIONS

Tin oxide (SnO_2) nanocrystallites and thin film were synthesized successfully by Sol-Gel method. Here, we conclude from XRD analysis that particles are polycrystallized with tetragonal rutile structure. Morphological characteristics of SnO_2 nanocrystallines thin film are obtained from SEM image, shows uniform distribution of quite a small grains with average crystallite size of 52 nm. The absorbance and transmittance spectra shows that synthesized tin oxide nanoparticles were smaller in size and homogenous. Uv-Vis analysis showed the characteristic absorbance peak at $\lambda = 312$ nm for SnO_2. The bandgap of SnO_2 nanoparticles was measured from the plot of variation of $(\alpha h\nu)^2$ versus $h\nu$ was 3.78 eV. The transmittance analysis showed the transmittance of 78 % for as synthesized SnO_2 thin film in the spectral range 350 nm to 800 nm.

ACKNOWLEDGEMENTS

The authors wish to thank for the support extended by the Management, Director, Vishwakarma Institute of Technology and Head, Department of Engineering Sciences and Humanities (DESH), VIT Pune.

REFERENCES

1. Z. Ying, Q. Wan, Z. Song, S. Feng, *Nanotechnology* **15** No 11, 1682 (2004).
2. A. Singh, U. Nakate, *Adv. Nanoparticles* **2**, 66 (2013).
3. Y.H. Chiu, C. Yeh, *J. Phys. Chem. C* **111** No 20, 7256 (2007).
4. A. Firooz, A. Mahjoub, A. Khodadadib, *Mater. Lett.* **62** No 12-13, 1789 (2008).
5. E. Leite, I. Weber, E. Longo, J. Varela, *Adv. Mater.* **12** No 13, 965 (2000).
6. C. Nayral, E. Viala, P. Fau, F. Senocq, J. Jumas, A. Maisonnat, B. Chaudret, *Chem. Eur. J.* **6** No 22, 4082 (2000).
7. J. Zhu, Z. Lu, S. Aruna, D. Aurbach, A. Gedanken, *Chem. Mater.* **12** No 9, 2557 (2000).
8. G. Pang, S. Chen, Y. Koltypin, A. Zaban, S. Feng, A. Gedanken, *Nano Lett.* **1** No 12, 723 (2001).
9. V. Subramanian, W. Burke, H. Zhu, B. Wei, *J. Phys. Chem. C* **112** No 12, 4550 (2008).
10. J. Jouhannaud, J. Rossignol, D. Stuerga, *J. Solid State Chem.* **181** No 6, 1439 (2008).
11. Y. Wang, C. Ma, X. Sun, H. Li, *Nanotechnology* **13** No 5, 565 (2002).
12. P. Baker, R. Sanderson, A. Crouch, *Thin Solid Films* **515** No 17, 6691 (2007).
13. S. Gnanam, V. Rajendran, *Dig. J. Nanomater. Biostruct.* **5** No 3, 699 (2010).
14. H. Klug, L. Alexander, *X-Ray Diffraction Procedures: For Polycrystalline and Amorphous Materials* (New York, USA: John Wiley and Sons: 1974).
15. R. Swarnkar, S. Singh, R. Gopal, *Bull. Mater. Sci.* **34** No 7, 1363 (2011).
16. A. Azam, S. Habib, N. Salah, F. Ahmed, *Int. J. Nanomedicine* **8** No 1, 3875 (2013).